Marc Röger
German Aerospace Center (DLR),
Institute of Solar Research,
Plataforma Solar de Almería,
Tabernas 04200, Spain
e-mail: marc.roeger@dlr.de

Peter Potzel
Institute of Thermodynamics and Thermal
Engineering (ITW),
University of Stuttgart,
Stuttgart 70550, Germany

Johannes Pernpeintner
German Aerospace Center (DLR),
Institute of Solar Research,
Cologne 51147, Germany

Simon Caron
German Aerospace Center (DLR),
Institute of Solar Research,
Plataforma Solar de Almería,
Tabernas 04200, Spain

A Transient Thermography Method to Separate Heat Loss Mechanisms in Parabolic Trough Receivers

This paper describes a transient thermography method to measure the heat loss of parabolic trough receivers and separate their heat loss mechanisms. This method is complementary to existing stationary techniques, which use either energy balances or glass envelope temperature measurements to derive overall heat losses. It is shown that the receiver heat loss can be calculated by applying a thermal excitation on the absorber tube and measuring both absorber tube and glass envelope temperature signals. Additionally, the emittance of the absorber selective coating and the vacuum quality of the annulus can be derived. The benefits and the limits of the transient method are presented and compared to the established stationary method based on glass envelope temperature measurements. Simulation studies and first validation experiments are described. A simulation based uncertainty analysis indicates that an uncertainty level of approximately 5% could be achieved on heat loss measurements for the transient method introduced in this paper, whereas for a conventional stationary field measurement technique, the uncertainty is estimated to 17–19%. [DOI: 10.1115/1.4024739]

Keywords: parabolic trough receiver, heat loss measurement, transient thermography, numerical modeling, uncertainty analysis

1 Introduction

Solar thermal parabolic trough plants concentrate the sunlight on receiver tubes, which absorb the solar radiation and transfer the thermal energy to a heat transfer fluid (e.g., thermal oil, water, and molten salt). The receivers usually consist of a steel receiver tube coated with a selective coating having high solar absorptance and low thermal emittance. The steel receiver tube is surrounded by a concentric glass envelope tube to maintain a vacuum in the annulus between the two tubes, and hence reduce convective losses. The steel and glass envelope are connected at their ends with metal-glass bellows which have to compensate for the different thermal expansions of steel and glass and temperature difference between the two materials. A getter material is placed inside the vacuum space to maintain the vacuum in case of residual gas or small amounts of hydrogen permeating from the thermofluid to the annulus.

In molten salt parabolic trough plants, the actual receivers are operated up to about $580\,°C$. In plants using thermal oil as heat transfer fluid, they are limited to about $400\,°C$. Receiver heat loss plays an important role in the thermal and economic performance of a concentrated solar power plant. The heat loss of an evacuated parabolic trough receiver (PTR) ranges typically between 150 or below and $200\,W/m$ for a receivers with $70\,mm$ steel tube diameter at $350\,°C$ [1,2]. This heat loss value can get five or ten times higher if hydrogen permeates into the receiver annulus. If several receivers in a power plant are defective (e.g., vacuum loss, glass breakage, and coating degradation), the annual electricity production decreases according to the higher thermal loss and the power plant economic performance is affected. Reliable measurement

techniques hence are relevant to be developed in order to assess the quality of receiver tubes installed in solar fields.

A laboratory measurement technique based on steady state Joule heating has been applied for single receiver tubes by National Renewable Energy Laboratory (NREL) [1,2], German Aerospace Center (DLR) [3], and Schott [4]. Various commercially available receivers have been successfully examined with this technique. Usually, the heat loss of already installed receivers is derived by infrared imaging of the glass envelope [5]. Due to the strong influence of ambient conditions such as ambient temperature, wind speed, sky, and ground temperature, this technique has a relatively large measurement uncertainty.

This paper presents a measurement method for parabolic trough receiver heat losses that is based on transient thermography. Transient thermography as applied here uses the observation how a periodic change in the steel temperature tube affects the glass envelope temperature. By measuring the temperature of steel and glass tube over time, and the mean ambient temperature, the heat loss, vacuum quality and emittance of the selective coating can be derived. This suggested method, implemented in the solar field, has the potential of significantly lower measurement uncertainty in comparison to existing stationary techniques. Furthermore, this transient method potentially gives the possibility to distinguish receiver heat loss mechanisms. Hence, this method can provide an insight into receiver degradation mechanisms as for instance the decomposition of the absorber selective coating or the loss of annulus vacuum, due to hydrogen permeation or air infiltration in the annulus.

Simulation studies and first validation experiments carried out on a single receiver tube under laboratory conditions are presented in this paper. The aim of this research is to develop a reliable heat loss measurement method to assess the performance properties of receiver tubes that are already installed in a solar field. The transient method should be seen as a complement to already existing stationary measurement techniques. The existing field measurement technique, which derives the heat loss of a receiver based on

glass envelope temperatures, is proposed for a comprehensive solar field screening and a rough classification of receivers according to their quality level. The transient method is intended to be applied for a more detailed and quantitative heat loss measurement of individual receiver tubes.

2 Transient Measurement Principle

The receiver consists basically of a coated steel absorber tube and a surrounding concentric cylindrical glass envelope. To derive the measurement principle, the receiver is modeled as a simplified dynamic heat transfer system, shown in Fig. 1. The steel absorber tube of temperature T_a and emittance ε_a and the glass envelope of temperature T_g and emittance ε_g are separated by an annulus, which can be characterized by a heat transfer coefficient h_{ann}. This system can be regarded as a thermal resistance network, which interacts with the ambient and the heat transfer fluid (HTF) flowing inside the absorber tube. The aim of a transient measurement is to identify unknown system parameters of interest, i.e., the emittance of the absorber ε_a and the annulus heat transfer coefficient h_{ann}.

As radiation is a major heat transfer mechanism, the system response is expected to be nonlinear with temperature. However, the system response can be linearized around a working point, if the temperature variations of steel absorber and glass envelope are small enough. Linear time-invariant system theory can then be applied.

Transient thermography uses the observation how a change in the steel temperature tube propagates to the glass envelope temperature. By applying a periodic thermal excitation on the absorber tube $T_a(t)$ and logging the temperatures $T_a(t)$, $T_g(t)$, and T_{amb}, the receiver heat loss properties can be derived. The absorber and glass temperatures are measured on their respective outer surfaces using IR thermography. Further system properties such as geometrical dimensions, thermal heat capacity, thermal conductivity, and glass envelope thickness must be known. If the absorber tube excitation signal is a cosine of small amplitude, the glass envelope temperature response is a cosine function of identical angular frequency, but of different amplitude and phase angle. In principle, any input function $T_a(t)$ can be used for system analysis, as long as this function contains frequencies for which the receiver system is sensitive, with respect to the unknown parameters defined above.

In case of a sinusoidal excitation, one can easily derive an amplitude ratio A and a phase angle φ based on the absorber and glass envelope temperature measurements. The amplitude ratio A is defined as the ratio between the glass temperature and the absorber temperature amplitudes. The phase angle φ is defined as the delay between the glass temperature and the absorber temperature signals. The amplitude ratio and the phase angle responses
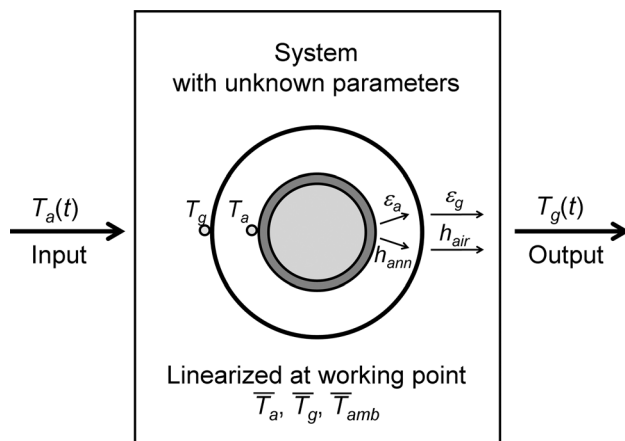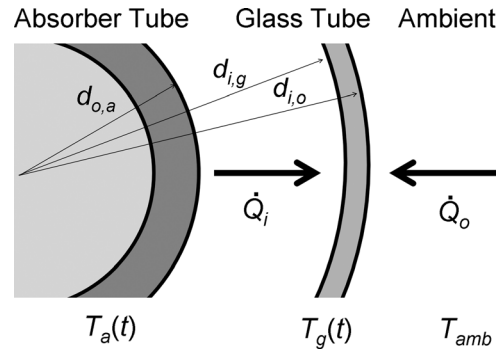

Fig. 2 Sketch of the lumped capacitance model for the glass envelope tube

both depend on the thermal resistance between the absorber tube and the glass envelope as well as on the thermal resistance between the glass envelope, and the ambient for a given excitation frequency ω and other boundary conditions such as receiver dimensions, material thermal properties, and operating conditions.

For future solar field applications, the absorber tube excitation does not have to be a periodic function. An excitation might be generated by for example focusing or defocusing upstream solar collectors or by varying the HTF temperature of the loop inlet.

In this section, a simplified analytical model is presented to gain a better understanding of the relationship between the receiver unknown parameters and the relevant measurands for the transient measurement technique. The simplified modeling approach consists in deriving a linearized lumped capacitance model for the glass envelope (see Fig. 2). Glass envelope temperature variations are neglected over the radial, circumferential and axial directions and heat transfer equations are linearized. The geometrical dimensions and material properties (ρ, c_p) of the glass envelope are given.

The transient energy balance for the glass envelope is

$$\rho c_p V \frac{dT_g}{dt} = \dot{Q}_i + \dot{Q}_o \tag{1}$$

The glass envelope temperature variation dT_g/dt is related to the heat flows at the inner and outer glass envelope surfaces $\dot{Q}_i$ and $\dot{Q}_o$, as illustrated in Fig. 2. Both heat flows can be described over a wide range of temperatures as the sum of a linear and a nonlinear temperature difference terms

$$\frac{\dot{Q}_i}{A_{i,g}} = b_{i,conv}\left(T_a - T_g\right) + b_{i,rad}\left(T_a^4 - T_g^4\right) \tag{2}$$

$$\frac{\dot{Q}_o}{A_{o,g}} = b_{o,conv}\left(T_{amb} - T_g\right) + b_{o,rad}\left(T_{amb}^4 - T_g^4\right) \tag{3}$$

with $A_{i,g} = \pi d_{i,g} L$ and $A_{o,g} = \pi d_{o,g} L$, while L being the receiver length. The glass envelope is approximated to be opaque for the relevant infrared wavelength range, so that the radiative heat transfer between the absorber and the ambient is neglected.

Linearization using a first order Taylor approximation can be considered as a good approximation in the vicinity of a specific working point, defined by the mean absorber and glass temperatures (respectively $\overline{T}_a$ and $\overline{T}_g$) under stable ambient conditions ($\overline{T}_{amb}$)

$$\frac{\dot{Q}_i}{A_{i,g}} \approx c_{i,a}(T_a - \overline{T_a}) + c_{i,g}(T_g - \overline{T_g}) \tag{4}$$

$$\frac{\dot{Q}_o}{A_{o,g}} \approx c_{o,g}(T_g - \overline{T_g}) \tag{5}$$

Fig. 1 Heat transfer system overview

The coefficients $c_{i,a}$, $c_{i,g}$, and $c_{o,g}$ are related to the four parameters $b_{i,conv}$, $b_{i,rad}$, $b_{o,conv}$, and $b_{o,rad}$ as well as the mean temperatures $\overline{T}_a$ and $\overline{T}_g$, according to the following equations:

$$c_{i,a} = b_{i,conv} + 4b_{i,rad} \cdot \overline{T}_a^{\,3} \qquad (6)$$

$$c_{i,g} = -\left(b_{i,conv} + 4b_{i,rad} \cdot \overline{T}_g^{\,3}\right) \qquad (7)$$

$$c_{o,g} = -\left(b_{o,conv} + 4b_{o,rad} \cdot \overline{T}_g^{\,3}\right) \qquad (8)$$

Introducing Eqs. (4) and (5) into Eq. (1), the linear time invariant system is described by

$$\rho c_p V \frac{dT_g}{dt} \approx A_i c_{i,a}(T_a - \overline{T_a}) + (A_i c_{i,g} + A_o c_{o,g})(T_g - \overline{T_g}) \qquad (9)$$

To solve Eq. (9), for a harmonic signal of the absorber temperature, we can write

$$T_a(t) = \overline{T_a} + \hat{T}_a e^{j(2\pi/T_{period})t} \qquad (10)$$

$$T_g(t) = \overline{T_g} + \hat{T}_g e^{j\left((2\pi/T_{period})t + \phi\right)} \qquad (11)$$

The differential equation can be solved by either inserting Eqs. (10) and (11) into Eq. (9) or by applying a Laplace transform on both sides of Eq. (9). Then, the frequency response $F(\omega)$ of the system is

$$F(\omega) = \frac{A_{i,g} c_{i,a}}{j\rho c_p V \omega - (A_{i,g} c_{i,g} + A_{o,g} c_{o,g})} \qquad (12)$$

The amplitude ratio $A(\omega)$ and the phase angle $\varphi(\omega)$ are

$$A(\omega) = \frac{\hat{T}_g}{\hat{T}_a} = |F(\omega)| = \frac{A_{i,g} c_{i,a}}{\sqrt{(\rho c_p V \omega)^2 + (A_{i,g} c_{i,g} + A_{o,g} c_{o,g})^2}} \qquad (13)$$

$$\phi(\omega) = \arg(F(\omega)) = \arctan\left(\frac{\rho c_p V \omega}{A_{i,g} c_{i,g} + A_{o,g} c_{o,g}}\right) \qquad (14)$$

Under quasi steady state conditions and for small oscillations of T_a and T_g, the time averaged inner and outer heat flow rates can be approximated by

$$\frac{\overline{\dot{Q}_i}}{A_{i,g}} = b_{i,conv}\left(\overline{T_a} - \overline{T_g}\right) + b_{i,rad}\left(\overline{T_a}^{\,4} - \overline{T_g}^{\,4}\right) \qquad (15)$$

$$\frac{\overline{\dot{Q}_o}}{A_{o,g}} = b_{o,conv}\left(T_{amb} - \overline{T_g}\right) + b_{o,rad}\left(T_{amb}^{\,4} - \overline{T_g}^{\,4}\right) \qquad (16)$$

Using the time averaged form of energy balance Eq. (1), we can write

$$\overline{\dot{Q}_i} + \overline{\dot{Q}_o} = 0 \qquad (17)$$

If in the experimental setup, we guarantee that the net radiative heat flow between the glass envelope and the ambient can be considered as negligible, the following equation is valid:

$$b_{o,rad} \approx 0 \qquad (18)$$

Assuming the geometrical quantities $A_{i,g}$, $A_{o,g}$, δ, and V, the glass material properties ρ, c_p and the cycle duration T_{period} are known and we measure the quantities A, φ, $\overline{T}_a$, $\overline{T}_g$, and $\overline{T}_{amb}$, the system of the nine algebraic Eqs. (6)–(8), (13)–(18) can be solved unambiguously to get the nine remaining unknowns $\dot{Q}_i$, $\dot{Q}_o$, $b_{i,conv}$, $b_{i,rad}$, $b_{o,conv}$, $b_{o,rad}$, $c_{i,a}$, $c_{i,g}$, and $c_{o,g}$. This system of equations has

been solved with computer algebra software. Details are skipped in this paper.

Equation (18) is valid, if a reflective shield (described in Sec. 4) is mounted around the receiver to reflect the thermal radiation emitted from the glass envelope back to itself for the purpose of the measurement. Thermal convection then becomes the dominant heat transfer mechanism at the outer surface of the glass envelope. Alternatively, the nonlinearity of the radiative flow between the glass envelope and the ambient can also be neglected, if the temperature difference between the ambient and the glass envelope does not exceed 50 K. In this case, the deviation between a linear heat loss correlation and the sum of convective and radiative heat loss is below 0.5% for typical ambient temperatures.

The annulus heat transfer coefficient h_{ann} and the absorber emittance ε_a are, respectively, related to parameters $b_{i,conv}$ and $b_{i,rad}$. Assuming that (i) the glass envelope is opaque to thermal radiation and (ii) the annulus gas does not absorb thermal radiation, the radiative heat transfer between the absorber tube and the glass envelope $\dot{Q}_{rad,a-g}$ is expressed in Eq. (19) according to [6]

$$\dot{Q}_{rad,a-g} = \frac{\pi d_{o,a} L \varepsilon_a \varepsilon_g \sigma}{\varepsilon_g + \varepsilon_a \cdot \left(1 - \varepsilon_g\right)\dfrac{d_{o,a}}{d_{i,g}}} \cdot \left(T_a^4 - T_g^4\right) \qquad (19)$$

By identifying $\dot{Q}_{rad,a-g}$ with the nonlinear temperature term of Eq. (2) and introducing receiver geometrical dimensions, it yields

$$\dot{Q}_{rad,a-g} = b_{i,rad}\left(\pi d_{i,g} L\right) \cdot \left(T_a^4 - T_g^4\right) \qquad (20)$$

The absorber emittance ε_a is hence related to $b_{i,rad}$ according to below equation

$$\varepsilon_a = \frac{\varepsilon_g}{\dfrac{d_{o,a}}{d_{i,g}}\left(\dfrac{1}{b_{i,rad}}\varepsilon_g \sigma + \varepsilon_g - 1\right)} \qquad (21)$$

The annulus heat flow, which is either due to gas heat conduction or natural convection, is here symbolized by $\dot{Q}_{conv,ann}$

$$\dot{Q}_{conv,ann} = h_{ann} \cdot \pi d_{o,a} L \cdot \left(T_a - T_g\right) \qquad (22)$$

By identifying $\dot{Q}_{conv,ann}$ with the linear temperature term of Eq. (2) and introducing receiver geometrical dimensions, we get

$$\dot{Q}_{conv,ann} = b_{i,conv}\left(\pi d_{i,g} L\right) \cdot \left(T_a - T_g\right) \qquad (23)$$

The annulus heat transfer coefficient h_{ann} is

$$h_{ann} = b_{i,conv}\frac{d_{i,g}}{d_{o,a}} \qquad (24)$$

The absorber emittance ε_a and the annulus heat transfer coefficient h_{ann} (and the heat loss $\dot{Q}'_{loss}$) can thus be derived from the five measurands A, φ, $\overline{T}_a$, $\overline{T}_g$, and T_{amb} by either using the simplified lumped parameter model or lookup tables created with a more sophisticated numerical model present in Sec. 3.

It may be worth noting that the convective heat transfer coefficient h_{air} to the surrounding air can also be determined experimentally. By applying a similar reasoning as presented above for the annulus heat transfer coefficient h_{ann}, one can identify h_{air} with $b_{o,conv}$. For this reason, we do not need any knowledge about the wind speed or air speed inside the radiation shield during a transient measurement.

Figure 3 shows amplitude and phase response of five parabolic trough receivers having different performance parameters plotted in polar coordinates on a 2D complex plane. As amplitude and phase response change as a function of air velocity, one receiver
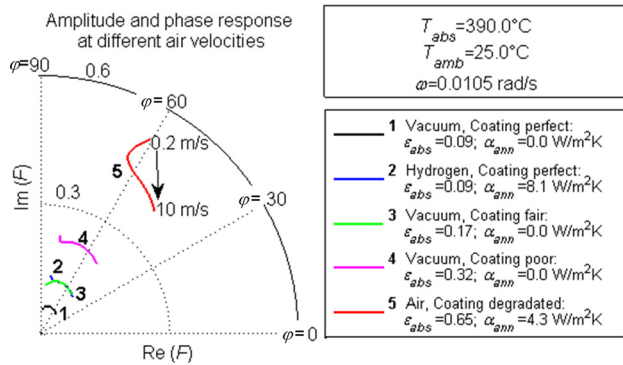
Fig. 3 Simulation results for five receivers with different characteristics under various external air velocities ranging from 0.2 to 10 m/s
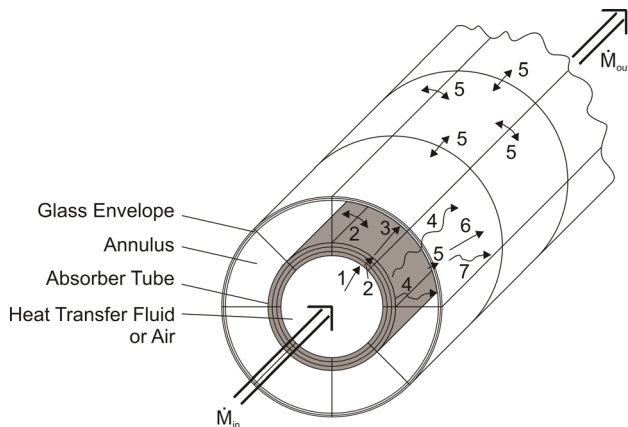

Fig. 4 Illustration of the three-dimensional model discretization scheme, fluid mass flow, and heat transfer mechanisms, labeled from 1 to 7

is represented by a line. An unambiguous solution of the heat loss performance properties of a receiver is achieved by using all five measurands A, φ, $\bar{T}_a$, $\bar{T}_g$, and T_{amb}.

3 Numerical Model

A transient numerical model is programmed for parabolic trough receivers to demonstrate the measurement concept feasibility and optimize the measurement technique. The numerical model extends the two-dimensional steady-state physical model of Forristall [7] to a three-dimensional finite element transient model. The geometrical discretization of the receiver is illustrated in Fig. 4 along with HTF mass flow rates ($\dot{M}_{in}$ and $\dot{M}_{out}$) and heat transfer mechanisms (1–7). The absorber tube and the glass envelope are both discretized in cylindrical coordinates. This discretization scheme gives the possibility of applying nonsymmetric boundary conditions, such as a partial solar irradiation or a radiation exchange with the ground and/or the sky.

Energy balance equations are formulated in a transient form both for the absorber tube and the glass envelope. Heat transfer mechanisms are listed in Table 1 with their respective correlations, which are used in the numerical model [8–16]. The model is implemented in the object-oriented language Modelica [17] and run with the Dymola simulation environment.

The numerical model is designed to simulate laboratory experiments. The numerical model describes the active part of the receiver. Support brackets and bellows heat losses are not taken into account by this model. Heat losses at receiver end faces of the steel and glass tubes are neglected, because, the ends are usually connected to other receiver end faces and they can be approximated as adiabatic surfaces. Simulation results are shown in Fig. 5 for two annulus degradation scenarios: (i) hydrogen permeation from the HTF through the absorber tube and (ii) air infiltration from the ambient through the glass envelope. The glass temperature is variable and changes according to the degradation scenarios.

One can identify three gas heat conduction regimes in Fig. 5. At low pressure (i.e., below 10^{-6} bar), gas heat conduction is linearly dependent on gas pressure (free molecular regime). For pressure from 10^{-6} bar to 10^{-3} bar, gas heat conduction increases in a nonlinear fashion (transition regime). For pressure from 10^{-3} bar

Table 1 Heat transfer mechanisms and their correlations for the numerical model

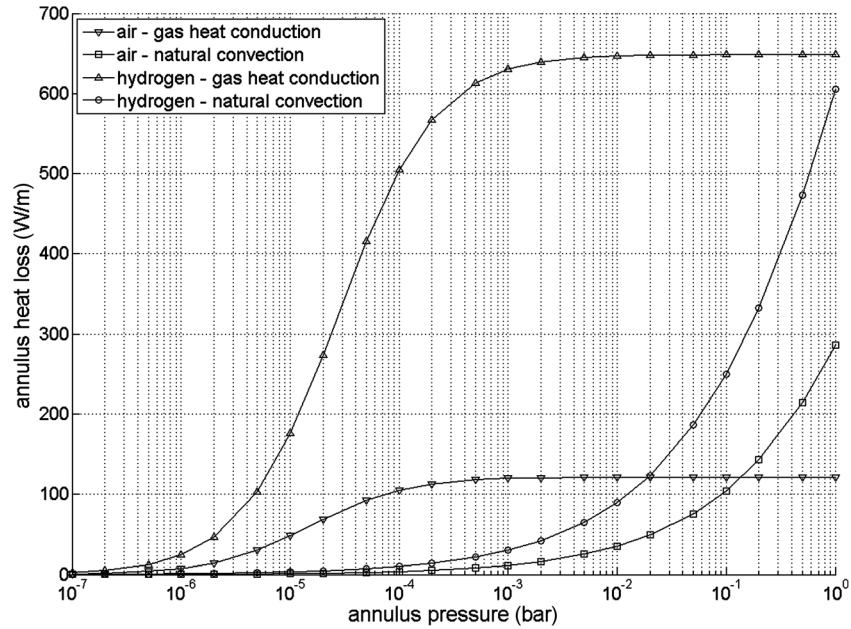| From	To	Heat transfer mechanism	Correlations and comments
HTF	Inner absorber surface	Convection (1)	Nusselt correlation, turbulent regime, Gnielinski [8]
Inner absorber surface	Outer absorber surface	Conduction (2)	Fourier's law of heat conduction
			Steel material [2]
Outer absorber surface	Inner glass surface	Gas conduction or convection (3)	Gas heat conduction:
			Correlation from Ratzel et al. [9], additional data and correlations taken from Ref. [8–14]
			Natural convection:
			Bejan correlation [15]
Outer absorber surface	Inner glass surface/ ambient	Radiation (4)	Annulus radiation heat exchange between absorber tube and glass envelope [16]
			Approximation of radiation emitted by the absorber tube and transmitted through glass envelope
Inner glass surface	Outer glass surface	Conduction (5)	Fourier's law of heat conduction
			Glass material
Outer glass surface	Ambient	Convection (6)	No wind (<0.1 m/s):
			Nusselt correlation, Churchill and Chu [6]
			Wind (>0.1 m/s):
			Nusselt correlation, Zukauskas [6]
Outer glass surface	Ambient	Radiation (7)	Radiation heat exchange between glass envelope and ambient [16]

Fig. 5 Annulus heat loss (gas heat conduction and natural convection) at different annulus pressures for a PTR 70. $T_a = 350\,°C$, $T_{amb} = 25\,°C$; T_g variable, wind 0 m/s

to 1 bar, gas heat conduction is no longer a function of gas pressure (continuum regime [18,19]).

The transition from gas heat conduction to natural convection depends on the Rayleigh number Ra. The critical Ra value for annulus geometry is approximately 1000 [9]. Since a precise transition criterion between gas heat conduction and natural convection cannot be defined, the annulus heat loss is conservatively estimated by taking the maximum of gas heat conduction and natural convection heat loss values.

The numerical model is validated against a NREL heat loss measurement dataset obtained for two Schott PTR 70 receiver tubes [2] tested on NREL's parabolic trough receiver test bench at test temperatures from 100 °C to 500 °C. The uncertainty on the receiver heat loss was estimated by NREL to ±10 W/m, the uncertainty on the glass envelope temperature to ±20 K [2] corresponding to the test conditions with slightly different air speeds.

Figure 6 shows heat loss and glass temperatures from NREL measurements. Simulation results of the numerical model assume the following correlation for the absorber emittance: $\varepsilon_a = 2 \times 10^{-7} \cdot T_a^2 + 0.062$ [2].

4 Experimental Setup

To fulfill Eq. (18) and ensure negligible net radiative heat flow between the receiver glass envelope and the ambient, a radiation shield is used (Fig. 7). It reflects the thermal radiation emitted from the glass envelope back to itself. The remaining convective heat transfer mechanism between the glass envelope and the ambient can be approximated as a linear phenomenon. The radiation shield consists of two hollow half cylinders assembled together around the receiver tube. The length of these half cylinders is about 1 m to ensure the radiative conditions at the measurement point. The inner wall of these half cylinders is covered with an IR reflecting sheet. Small fans are mounted on one side of the radiation shield to ventilate the annulus between the glass envelope and the radiation shield in order to avoid a heat build-up. The absorber and the glass envelope temperatures are measured with IR thermography through a small aperture in the radiation shield.

A performance test is carried out to assess the IR reflection sheet used in the radiation shield. The infrared camera measured the glass temperature directly (57 °C) and by using the reflection of the hot glass on the reflection sheet (53 °C). According to the Stefan–Boltzmann law, the temperature difference of 4 K means that 95% of the thermal radiation emitted by the glass envelope tube is reflected back to itself. The net radiative heat flow from the glass envelope to the radiation shield can hence be neglected
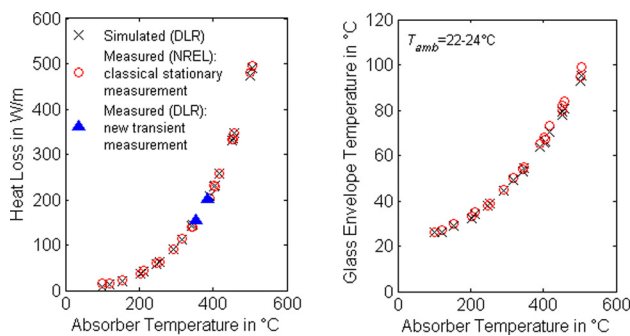

Fig. 6 Receiver heat loss (left) and glass envelope temperature (right). Comparison of NREL experimental data [2] (circle) with simulation results (numerical model, Sec. 3, cross) and experimental results (transient measurements, triangle) for an intact Schott PTR 70 receiver.
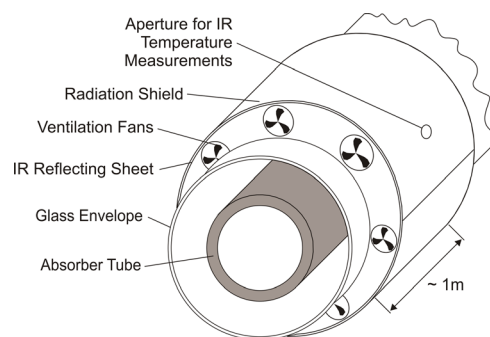

Fig. 7 Radiation shield design

in comparison to the convective flow in the gap between the glass envelope and the radiation shield.

For the laboratory setup, a Schott PTR 70 receiver is heated by applying a high electric current through the absorber tube (Joule heating). The absorber tube and the glass envelope temperatures are measured with a Cedip Titanium IR camera and an Infratec VarioCam IR camera with appropriate optical filters. Type K thermocouples are installed on the inner absorber tube surface and on the outer glass envelope surface to calibrate emittance values for both IR cameras.

An appropriate cycle period has to be chosen for the sinusoidal thermal excitation. If the period is too short, the glass temperature oscillations are strongly damped and the phase response is not sensitive. If the period is too long, the phase response is not sensitive and the measurement time is too long. For commercially available receivers with 2 mm absorber tube thickness and 3 mm glass tube thickness, cycle durations between 600 s and 2000 s are recommended. As measurement time should be minimum, a cycle duration of 600 s is set for laboratory experiments.

5 Data Evaluation

A look-up table is generated to obtain the output values ε_a and h_{ann} from the five measurands $A, \varphi, \bar{T}_a, \bar{T}_g$, and T_{amb}. This look-up table is generated using the numerical model presented in section 3 with the laboratory setup boundary conditions described in Sec. 4. The net radiative heat flow from the glass envelope to the ambient is set to zero and there is no HTF flowing through the absorber tube. The temperature distribution on the outer absorber surface is assumed to be uniform and the absorber temperature is given as a boundary condition. Several scenarios are simulated with the numerical model to fill the look-up table, taking into account a wide variation of (i) receiver conditions (absorber emittance, annulus pressure, and annulus filling with hydrogen), (ii) test conditions (outer absorber surface temperature) and (iii) environmental conditions (wind speed and ambient temperature). A latin hypercube sampling method is adopted to create a representative set of input parameter values from this multidimensional space.

For these simulations, the outer absorber temperature is defined as a cosine function with an amplitude of 10 K and a period of 600 s. After each simulation run, the amplitude ratio A and the phase shift angle φ are computed and stored with the mean

absorber temperature $\bar{T}_a$, the mean glass temperature $\bar{T}_g$, the ambient temperature T_{amb}, and the obtained receiver parameters ε_a and h_{ann} in the look-up table.

The receiver heat loss $\dot{Q}_{loss}$ is then calculated with the help of a new simulation run, using the derived parameter values ε_a and h_{ann} along with the desired boundary conditions, e.g., specific field boundary conditions or standardized laboratory conditions.

The thermal quality of a parabolic trough receiver can be alternatively quantified by a UA_L value, which is the product of an overall heat transfer coefficient U (Units: W/m^2 K) and the ratio A_L of the receiver area A (Unit: m^2) to the receiver length L (Unit: m). The UA_L value (Units: W/m·K) is calculated by normalizing the receiver heat loss $\dot{Q}_{loss}$ (W) per unit receiver length L and then by dividing the receiver heat loss per unit length $\dot{Q}'_{loss}$ (W/m) by the temperature difference between the absorber tube and the glass envelope

$$UA_L = \frac{\dot{Q}'_{loss}}{T_a - T_g} \qquad (25)$$

The temperature difference is defined from the outer absorber surface temperature T_a to the outer glass envelope surface temperature T_g. These temperatures are chosen because they are the driving force for the receiver heat loss and both surface temperatures can be measured with noncontact IR thermography. Moreover, the heat loss $\dot{Q}'_{loss}$ (W/m) changes considerably for degraded tubes with varying wind speeds whereas the changes of UA_L (W/m K) are significantly smaller.

6 Method Validation

Four experimental measurements are presented in order to provide a validation of the findings based on simulations. Table 2 gives an overview of the validation measurements performed on an intact PTR 70 receiver. The receiver dynamic behavior is studied under various experimental conditions. Variations are applied to the mean absorber temperature, the ventilation air velocity and the cycle duration. The radiation shield ventilation air velocity is set at a low value (respectively, medium value) for experiments 1 and 2 (respectively, experiments 3 and 4).

Table 2 Summary of experiments (*a*), measurands (*b*), results (*c*) carried out with the transient method on an evacuated PTR 70 receiver, and simulation results (*d*). Heat loss is reported for a mean absorber temperature $T_a = 350\,^{\circ}$C and laboratory conditions.

	1	2	3	4	Reference[a,b]
(a) Experiment					
Experiment number	1	2	3	4	Reference[a,b]
Absorber temperature T_a	Medium	High	High	High	350 °C
Cycle duration T_{period} (s)	600	600	600	300	—
Air velocity level	Low	Low	Medium	Medium	0 m/s
(b) Measurands					
Amplitude ratio response A	0.049	0.060	0.065	0.034	—
Phase angle response φ (rad)	−1.40	−1.44	−1.42	−1.53	—
Mean absorber temperature $\bar{T}_a$ (°C)	353	386	386	383	350
Mean glass temperature $\bar{T}_g$ (°C)	78	91	85	85	—
Mean ambient temperature $\bar{T}_{amb}$ (°C)	24	24	24	24	24
(c) Evaluation					
Absorber emittance ε_a (—) at $\bar{T}_a$	0.093	0.091	0.096	0.094	0.087
Annulus heat transfer h_{ann} (W/m^2 K)	0.1	0.1	0.0	0.1	0.0
Heat loss $\dot{Q}'_{loss}$ (W/m) at 350 °C[b]	166	153	158	162	150
UA_L (W/m K) at 350 °C[b]	0.57	0.52	0.54	0.55	0.51
Heat loss deviation between experimental and reference data[b]	+10.7%	+2.0%	+5.3%	+8.0%	0.0%
(d) Simulation results of numerical model using data of reference receiver[a]					
Amplitude ratio response A	0.053	0.061	0.062	0.031	—
Phase angle response φ (rad)	−1.44	−1.44	−1.43	−1.52	—
Mean glass temperature $\bar{T}_g$ (°C)	78	91	85	84	—

[a]PTR 70 receiver; modeling assumptions: $\varepsilon_a = 2 \times 10^{-7} \cdot T_a^2 + 0.062$ [2]; vacuum pressure 10^{-7} bar.
[b]350 °C and laboratory conditions (i.e., no wind, free convection, $T_{amb} = 24\,^{\circ}$C, without radiation shield).
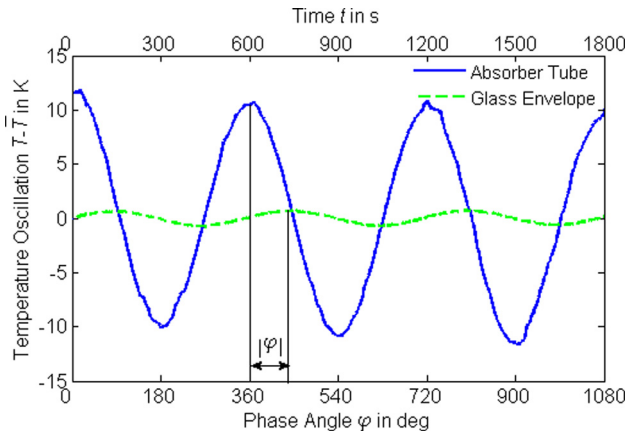
Fig. 8 Temperature oscillation measured for the absorber tube (continuous line) and the glass envelope (dashed line) during the experiment 2 ($\bar{T}_a = 386\,°C$; $\bar{T}_g = 91\,°C$)

Figure 8 shows exemplarily the temperature oscillations of the absorber and glass tube of experiment 2 of Table 2. The absorber tube is operated at a mean temperature of 386 °C with an amplitude of about 10 K. The amplitude of the glass envelope temperature response is much smaller (0.6 K), because the tested receiver is new. A phase shift φ of 83 deg is measured between the two signals. The mean glass temperature of 91 °C is higher than for field mounted receivers because of the radiation shield.

In Table 2, part (b) shows the measurands and part (c) the evaluation of the PTR 70 receiver. The measurements result in a selective coating emittance ε_a in the range from 0.091 to 0.096 and in an annulus heat transfer coefficient h_{ann} in the range from 0.0 to 0.1 W/m²K for all four experiments.

The measurement results are compared to NREL reference PTR 70 data, assuming an absorber temperature of 350 °C, an ambient temperature of 24 °C, no wind and no radiation shield (Table 2, right column). The reference emittance ε_a is 0.087 and the annulus pressure is assumed to be 10^{-7} bar, which leads to $h_{ann} = 0.01$ W/m²K. The heat loss $\dot{Q}'_{loss}$ is always given for laboratory conditions at an absorber temperature of 350 °C and without radiation shield. The emittance values measured with the transient method differ because the absorber tube temperature was different in the four experiments. If we account for the temperature difference using

the correction correlation stated in Table 2 at the bottom, the difference to the reference value gets smaller.

The heat loss calculated with the numerical model and NREL reference PTR 70 data is 150 W/m at 350 °C absorber temperature. The estimate of the periodic transient measurement heat loss uncertainty is about 5%, assuming the following measurement uncertainties: ±2 K, ±0.5 K, and ±0.5 K for the absorber, glass, and ambient temperature, respectively, ±0.001 for the amplitude ratio response and ±0.01 rad for the phase angle response. The observed deviations in heat loss values between the experiments and reference data are, respectively, 11%, 2%, 5%, and 8%, for experiments 1–4. The deviations are above 5% for experiments 1 and 4, which exceed the predicted uncertainty level. For the first experiment, the measurement accuracy is negatively influenced by nonideal IR camera settings. This partly explains the higher measurement uncertainty observed for the first experiments. For the fourth experiment, the cycle duration T_{period} is reduced to 300 s, which is not optimal. The experiment yields similar results compared to the others but with a higher measurement uncertainty.

Additionally to the measurements, numerical simulations, assuming a perfect vacuum in the annulus and using the emittance correlation given by NREL [2], are reported in Table 2, part (d). Air velocity inside the radiation shield is adapted in the numerical model in a way that the simulated glass temperature is the same as the measured one. The low and medium air velocities assumed for the simulation are 0.81 m/s and 0.95 m/s for the low and medium air velocity level.

The simulated amplitude ratio A and the phase angle φ (Table 2, part (d)) are compared to experimental data (Table 2, part (b)) to provide some information about the uncertainties of these values for the uncertainty analysis. In general, a good agreement is observed. Experiment 1 shows the highest deviations. The deviations for experiments 2–4 are, respectively, ±0.001 to 0.003 (–) and ±0.01 rad for the amplitude ratio and the phase angle responses.

7 Uncertainty Analysis for Solar Field Applications

The measurement uncertainties of the transient and stationary techniques under field conditions, carried out for a new and an aged receiver, is performed according to the ISO Guide to the expression of uncertainty in measurement [20]. Ambient conditions, receiver characteristics and measurement uncertainties are reported in Table 3. The sky temperature is assumed to be 8 K below ambient temperature while the ground temperature is assumed to be 20 K above ambient temperature. The assumptions

Table 3 Comparative uncertainty analysis between transient and stationary heat loss measurement techniques based on the numerical model and GUM [20]

Measurement method	Stationary technique		Transient technique	
Receiver type	New	Degraded	New	Degraded
(a) Receiver and ambient conditions				
Absorber emittance ε_a	0.11	0.22	0.11	0.22
Annulus heat transfer h_{ann} (W/m²K)	0.0	1.2	0.0	1.2
Absorber temperature $\bar{T}_a$ (°C)	350		350	
Wind speed (m/s)	1		1	
Ambient temperature T_{amb} (°C)	35		35	
(b) Uncertainties of measurands				
Amplitude response A	—		±0.001	
Phase response φ (rad)	—		±0.01	
Absorber temperature $\bar{T}_a$ (K)	±15		±15	
Glass temperature $\bar{T}_g$ (K)	±0.5		±0.5	
Ambient temperature T_{amb} (K)	±0.5		±0.5	
Wind speed (m/s)	±0.5		—	
(c) Uncertainties in heat loss measurement				
Uncertainty in $\dot{Q}'_{loss}$ (%)	±19.1	±17.2	±5.3	±5.0
Uncertainty in UA_L (%)	±19.0	±17.1	±5.2	±4.7

made for measurand uncertainties are based on the experience gathered from different measurement campaigns. For a stationary technique, similar to the one exposed in Ref. [5], the wind speed should be measured as it is a significant disturbance value. For the transient technique, the air velocity in the annulus between the radiation shield and the glass envelope is not required, as it is implicitly taken into account. The influences of variable ambient, sky and earth temperatures are not included in this analysis.

For the stationary technique, the measurement uncertainty related to heat loss is estimated between 17% and 19%. The uncertainty given in Table 3 for wind speed is a rough estimate, which might be very difficult to achieve in real conditions near a receiver tube, except for very calm weather conditions. If the wind speed uncertainty doubles to ± 1 m/s, then the heat loss measurement uncertainty almost doubles. Wind speed is thus a highly sensitive disturbance value for stationary techniques.

For the transient technique, the uncertainties of the amplitude ratio and the phase angle responses are respectively assumed to be ± 0.001 (–) and ± 0.01 rad. These values seem to be plausible based on the first experiments. The measurement uncertainty related to heat loss figures is calculated to 5% for the transient technique. If the measurement uncertainty associated with the amplitude ratio response doubles, then the measurement uncertainty related to heat loss indicators is observed to increase by only 0.2%. If the measurement uncertainty on the phase angle response doubles from ± 0.01 rad to ± 0.02 rad, then the heat loss measurement uncertainty is expected to increase by 5% according to simulation results. The results of the transient technique are thus highly sensitive to phase angle response measurements.

8 Conclusion and Outlook

A transient technique is presented for the measurement of parabolic trough receiver heat losses. The heat loss can be derived by applying a periodic thermal excitation on the absorber tube and by measuring the temperatures of absorber tube, glass envelope and ambient. This nondestructive transient technique gives the possibility to determine the absorber selective coating emittance and the annulus heat transfer coefficient, hence providing valuable information about receiver degradation.

The measurement principle is developed and demonstration experiments have been carried out on an intact PTR 70 receiver under laboratory conditions. The relative heat loss measurement deviations ranged from 2.0% to 10.7%, in comparison to a reference NREL measurement campaign [2]. Further laboratory experiments in an enhanced test rig are in preparation to confirm the potential of this measurement technique.

The measurement method has potential to be applied to receivers installed in a parabolic trough solar field. The thermal excitation of the absorber tubes is achieved by either focusing or defocusing an upstream collector or by varying the HTF mass flow rate. The measurement time is expected to be in the range of 1 h. The method has shown significant potential for improving the heat loss measurement uncertainty for field measurements. The uncertainty of the transient measurement technique is estimated to be in the range from 5% to 10%. Using a conventional stationary field technique, the measurement uncertainty has been estimated to be in range of 17–19%.

The presented measurement technique is recommended for a more detailed characterization of individual receiver tubes while methods using the glass envelope tube temperature as indicator allow a fast screening for large field areas.

Nomenclature

A = surface area (m^2)
A = amplitude response
b = coefficient (physical model) (W/m^{2}K or W/m^2 K^4)
C = coefficient (linear approximation) (W/m^2 K)
c_p = specific heat capacity of glass (J/kg K)
d = diameter (m)
F = frequency response
h = convective heat transfer coefficient (W/m^2 K)
j = imaginary number
L = receiver length (m)
$\dot{M}_{in}$ = HTF mass flow rate (in)
$\dot{M}_{out}$ = HTF mass flow rate (out)
Q = heat flow (W)
T = temperature (K)
T_{period} = thermal excitation cycle duration (s)
V = volume (m^3)
v = velocity (m/s)
U = overall heat loss coefficient (W/m^{2}K)
A_L = Receiver area per unit length (m)

Greek Symbols

δ = glass envelope thickness (m)
λ = glass thermal conductivity (W/m K)
ρ = density of glass envelope (kg/m^3)
φ = phase response, phase shift/angle (deg/rad)
ω = angular frequency (rad/s)

Subscripts

a = absorber tube
air = air
amb = ambient
ann = receiver annulus
conv = convective/conductive
g = glass envelope
i = inner surface
loss = heat loss
o = outer surface
rad = radiative

Superscripts

$^{-}$ = mean value/steady state
$^{\wedge}$ = amplitude
$^{\prime}$ = per unit length

References

[1] Burkholder, F., and Kutscher, C., 2008, "Heat Loss Testing of Solel's UVAC3 Parabolic Trough Receiver," National Renewable Energy Laboratory Technical Report, NREL/TP-550-42394.

[2] Burkholder, F., and Kutscher, C., 2009, "Heat Loss Testing of Schott's 2008 PTR70 Parabolic Trough Receiver," National Renewable Energy Laboratory Technical Report, NREL/TP-550-45633.

[3] Lüpfert, E., Riffelmann, K.-J., Price, H., Burkholder, F., and Moss, T., 2008, "Experimental Analysis of Overall Thermal Properties of Parabolic Trough Receivers," ASME J. Sol. Energy Eng., 130, p. 021007.

[4] Dreyer, S., Eichel, P., Gnaedig, T., Hacker, Z., Janker, S., Kuckelkorn, T., Silmy, K., Pernpeintner, J., and Lüpfert, E., 2010, "Heat Loss Measurements on Parabolic Trough Receivers," SolarPACES 2010, Perpignan, France, September 21–24.

[5] Price, H., Forristall, R., Wendelin, T., Lewandowski, A., Moss, T., and Gummo, C., 2006, "Field Survey of Parabolic Trough Receiver Thermal Performance," Solar 2006 Conference (ISEC'06), Denver, CO, July 8–13, Paper No. NREL/CP-550-39459.

[6] Incropera, F., Dewitt, D., Bergman, T., and Lavine, A., 2007, Fundamentals of Heat and Mass Transfer, 6th ed., John Wiley & Sons, Inc., Hoboken, NJ.

[7] Forristall, R., 2003, "Heat Transfer Analysis and Modeling of a Parabolic Trough Solar Receiver Implemented in Engineering Equation Solver," National Renewable Energy Laboratory Technical Report No. NREL/TP-550-34169.

[8] Gnielinski, V., 2006, "Wärmeübertragung bei der Strömung durch Rohre," VDI-Wärmeatlas, 10th ed., Springer-Verlag, Berlin, Chap. Ga.

[9] Ratzel, A. C., Hickox, C. E., and Gartling, D. K., 1979, Techniques for Reducing Thermal Conduction and Natural Convection Heat Losses in Annular Receiver Geometries," ASME J. Heat Transfer, 101, pp. 108–113.

[10] Dudley, V. E., Kolb, G. J., Mahoney, A. R., Mancini, T. R., Matthews, C. W., Sloan, M., and Kearney, D., 1994, "Test Results SEGS LS-2 Solar Collector," Sandia National Laboratories, Report No. SAND94-1884.

[11] McBride, B. J., Zehe, M. J., and Gordon, S., 2002, "NASA Glenn Coefficients for Calculating Thermodynamic Properties of Individual Species," NASA Report No. TP-2002-211556.

[12] Kleiber, M., and Joh, R., 2006, "Stoffwerte von sonstigen chemisch einheitlichen Flüssigkeiten und Gasen," *VDI-Wärmeatlas*, 10th ed., Springer-Verlag, Berlin, Chapter Dca.

[13] Selle, S., 2002, "Transportkoeffizienten ionisierter Spezies in reaktiven Strömungen," Inaugural-Dissertation, Ruprecht-Karls-Universität, Heidelberg.

[14] Golovicher, L. E., Kolenchits, O. A., and Nesterov, N. A., 1989, "Dynamic Viscosity of Gases Over a Wide Range of Temperatures," J. Eng. Phys. Thermodyn., **56**(6), pp. 689–694.

[15] Bejan, A., 1995, *Convection Heat Transfer*, 2nd ed., Wiley, New York.

[16] Siegel, R., and Howell, J. R., 1981, *Thermal Radiation Heat Transfer*, 2nd ed., McGraw-Hill Book Company, New York.

[17] Tiller, M., 2001, *Introduction to Physical Modeling With Modelica*, Kluwer Academic Publishers, Norwell, MA.

[18] Burkholder, F., Kutscher, C., Brandemuehl, M., and Wolfrum, E., 2011, "The Test and Prediction of Argon-Hydrogen and Xenon-Hydrogen Heat Conduction in Parabolic Trough Receivers," SolarPACES 2011, Granada, Spain, September 20–23.

[19] Burkholder, F., 2011, "Transition Regime Heat Conduction of Argon/Hydrogen and Xenon/Hydrogen Mixtures in a Parabolic Trough Receiver," Ph.D. thesis, Department of Civil, Environmental, and Architectural Engineering, University of Colorado, Boulder, CO.

[20] International Organization for Standardization, 2008, "ISO/IEC Guide 98-3:2008: Uncertainty in Measurement—Part 3: Guide to the Expression of Uncertainty in Measurement (GUM)," International Organization for Standardization, Geneva.